Vitamin D Receptor: Ligand Recognition and Allosteric Network†

Keiko Yamamoto,*,‡ Daijiro Abe,§ Nobuko Yoshimoto,§ Mihwa Choi,‡ Kenji Yamagishi,|| Hiroaki Tokiwa,|| Masato Shimizu,§ Makoto Makishima,⊥ and Sachiko Yamada*,‡,§

Institute of Biomaterials and Bioengineering and School of Biomedical Sciences, Tokyo Medical and Dental University, 2-3-10 Kanda-Surugadai, Chiyoda-ku, Tokyo 101-0062, Department of Chemistry, Faculty of Science, Rikkyo University, 3-34-1 Nishi-ikebukuro, Toshima-ku, Tokyo 171-8501, and Department of Biochemistry, Nihon University School of Medicine, Oyaguchi-kamicho, Itabashi-ku, Tokyo 173-8610, Japan

Received August 11, 2005

To investigate the allosteric effects of ligands in the function of nuclear receptors, we performed exhaustive alanine scanning mutational analysis (ASMA) of the residues lining the ligand-binding pocket (LBP) of the human vitamin D receptor. The effects of ligands were examined in this system (termed two-dimensional (2D) ASMA) using 10 structurally and biologically characteristic ligands that included agonists, partial agonists, and a full antagonist. The results clearly revealed the role and importance of all the amino acid residues lining the LBP and the relationships between ligand binding and transcriptional potency. 2D ASMA indicated ligand-specific ligand−protein interactions, which have key importance in determining the transactivation potency of the ligand. Taking the results as a whole, we suggest a ligand-mediated allosteric network through which information from ligands is transmitted to the interfaces with protein cofactors and which was shown to be linked to part of the network found by statistical coupling analysis.

Introduction

The vitamin D receptor (VDR) is a member of the nuclear receptor (NR) superfamily and functions as a ligand-dependent transcriptional factor.[1,2] Ligand binding triggers allosteric communication of NRs by changing the structures and/or character of the interfaces between the dimer partner and protein factors. It causes dissociation of corepressors[3] that bind to the static activation function 2 (AF-2) surface that is composed of parts of helix 3 (H3), loop 3−4, and H4/5 plus H11, association with the heterodimer partner via the dimer interface, and recruitment of coactivators[4] to the AF-2 surface that is formed by folding back of H12 on the static AF-2. The X-ray crystal structures of a large number of NRs with various conformations[5] have been determined, and these have provided detailed insight into the mechanism of action of NRs, such as the distinct conformational differences of H12 among inactive,[6] active[7,8] and antagonist-bound suppressive conformations.[9,10] However, solely on the basis of the receptor crystal structure, it is difficult to recognize the subtle conformational differences that result when structurally distinct ligands bind to the receptor. Such small differences in structure and/or character caused by binding of different ligands may elicit different biological responses. It is well-known that the receptor affinity and transactivation potency of NR ligands are not proportional to each other, but as yet there has been no clear explanation of why this should be the case.[11]

Several approaches for identifying the structural determinants of allosteric activation of NRs have been reported. Shulman et al.[12] used statistical coupling analysis (SCA),[13] an approach in which evolution is regarded as a large-scale mutagenesis experiment with selection for function, and identified residues forming an allosteric network of NRs by analyzing the sequence homologies of all known NR proteins. However, this approach cannot be applied for investigating the allosteric effects of ligands on residues in the ligand-binding pocket (LBP), because the residues forming the LBP have been evolutionally selected to endow specificity for the cognate ligands for NRs. Greene's group[14,15] used the X-ray crystal structures of estrogen receptor (ER) subtypes complexed with synthetic ligands that show different transcriptional behaviors in the two ERs and, by detailed analysis, discovered the importance of the precise positioning of H11 to create a transcriptionally active conformation.

We planned to investigate the allosteric effects of NR ligands by analyzing the interactions between the residues lining the LBP and the ligands. For this purpose, we performed exhaustive alanine scanning mutational analysis (ASMA) of the LBP residues of the human vitamin D receptor (hVDR). The VDR is appropriate for this purpose because it has only one gene and one LBP isoform,[16] thus eliminating any complicating factors. We then extended the ASMA to a two-dimensional (2D) one that allowed the effects of mutations to be investigated bilaterally by varying the ligand.[17] We assumed that the LBP residues would be subject to different interactions upon binding of structurally distinct ligands, and that these different interactions would be manifested as different allosteric effects and, in turn, different biological responses. If it were possible to detect different receptor−ligand interactions, then this might shed light on the cause of the different actions of ligands. We have reported mutational analysis of some of the LBP residues (18),[17,18] but when considering the allosteric effects of ligands as a whole, exhaustive mutational analysis of the LBP residues is essential. Only an exhaustive (total) ASMA study can provide an answer to the question of how the effect of ligands is transmitted to the whole VDR via LBP residues. From total ASMA of the LBP residues (34 non-alanine residues) of the VDR-LBD (ligand-binding domain), we were able to understand the role and importance of each LBP residue and the relationship

† This paper is dedicated to Dr. Hector F. DeLuca on the occasion of his 75th birthday.

* To whom correspondence should be addressed. (K.Y.) Phone: +81 3 5280 8038. Fax: +81 3 5280 8005. E-mail: yamamoto.mr@tmd.ac.jp. (S.Y.) Phone: +81 426 64 1629. Fax: +81 426 64 1629. E-mail: yamada.vd@image.ocn.ne.jp.

‡ Institute of Biomaterials and Bioengineering, Tokyo Medical and Dental University.

§ School of Biomedical Sciences, Tokyo Medical and Dental University.

|| Rikkyo University.

⊥ Nihon University School of Medicine.

10.1021/jm050795q CCC: $33.50
Published on Web 01/21/2006

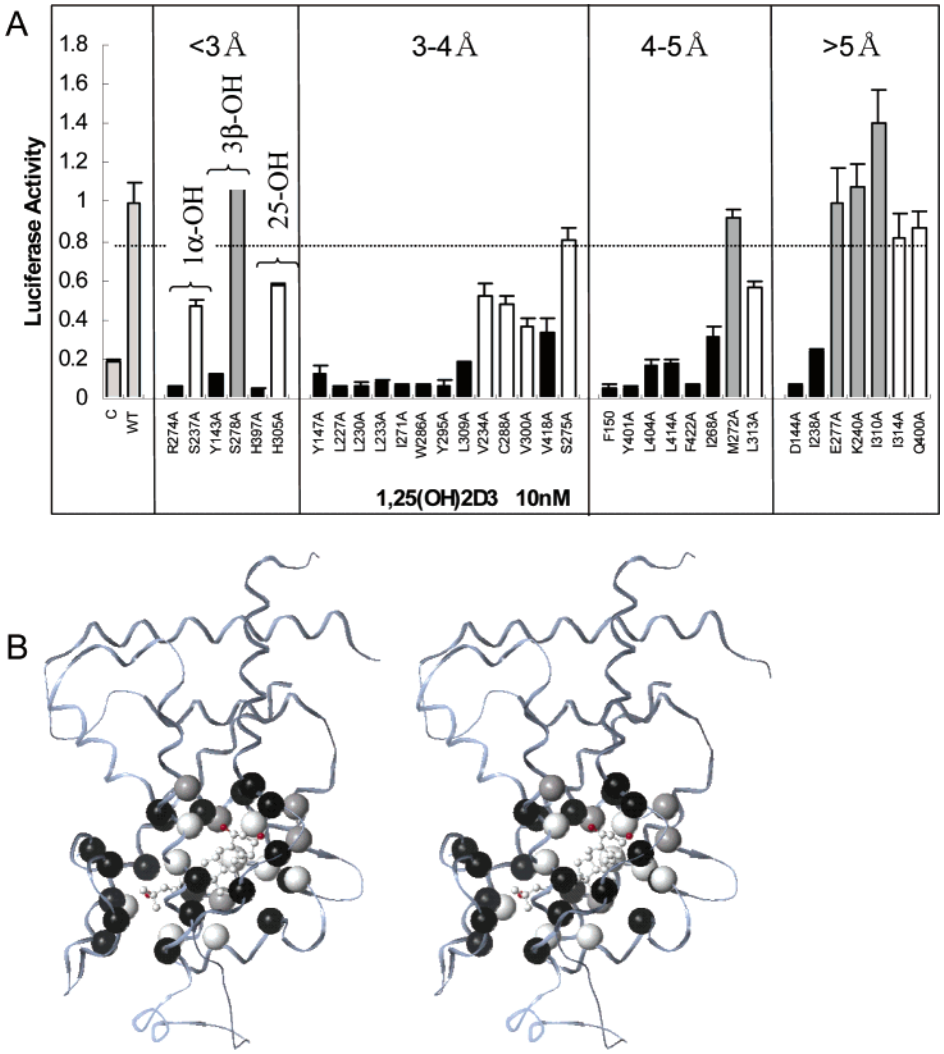

Figure 1. Transcriptional activities of one-point Ala mutants of 34 LBP non-alanine residues. (A) The activities were evaluated by dual luciferase assay using a full-length hVDR expression plasmid (pCMX-hVDR) and a luciferase reporter gene with a mouse osteopontin VDRE at the promoter (SPPx3-TK-Luc) in COS7 cells. Effects of mutation on the transactivation are discriminated by colors: black, mutation significantly reduced (<20%) the activity of the wild-type VDR (WT); white, mutation had a moderate effect (20−90%); gray, mutation had little effect or even elevated the potency (>90%). The percentage effects were corrected for the background activity (C) of endogenous VDR in COS7 cells. (B) Thirty-four non-alanine LBP residues of hVDR (stereoview). The non-alanine LBP residues are shown as balls at their Cα. The importance of each residue in the transactivation is designated with colors according to the results shown in (A).

between receptor affinity and transactivation. From the 2D total ASMA study, we were able to identify ligand-specific protein−ligand interactions that characterize the activity of the ligand. Finally, on the basis of our findings, we suggest a ligand-mediated allosteric network through which allosteric effects of ligands are transmitted to the surfaces with the dimer partner and coactivators. This ligand-mediated allosteric network was also shown to be linked to part of the SCA network found and reported by Shulman et al.[12]

Results and Discussion

1. Alanine Scanning Mutational Analysis. The hVDR-LBP is lined with 36 amino acid residues (34 non-alanine residues).[19−21] We prepared one-point Ala mutants for all 34 of the non-alanine LBP residues. The effects of Ala mutations on transactivation were evaluated by transient transcription assays using a full-length hVDR expression vector (pCMX-hVDR) and a luciferase reporter gene with the mouse osteopontin VDRE at the promoter (SPPx3-TK-Luc) in COS7 cells. The luciferase activities of all 34 mutants induced by $1,25(OH)_2D_3$ are summarized in Figure 1A, where the residues are grouped by the distances from the natural ligand ($1,25(OH)_2D_3$) in the X-ray crystal structure of hVDR-LBD (Protein Data Bank (PDB) entry 1db1). The results of total ASMA indicate that the effects of Ala mutations are not simply correlated with the distance from the ligand, but are diverse. The activities of half of the mutants were almost abolished or significantly reduced (<20% of the activity of the wild-type VDR), as shown by the black columns (Figure 1A). On the other hand, Ala mutations had little effect or even elevated the potency (>90%) for several residues, as shown by the gray columns. The remaining mutations had intermediate effects (clear columns). The 34 LBP residues are shown in the 3D structure of the VDR-LBD (Figure 1B) with the same color designation. We analyzed these results in more detail with respect to the distances of the residues from the ligand.

a. Residues within 3 Å from the Ligand. There are six residues within 3 Å, a hydrogen bond distance, from the three hydroxyl groups of $1,25(OH)_2D_3$ (Figure 1). The active vitamin D_3 has three OH groups, each of which has a pair of polar residues within a hydrogen bond distance: S237 and R274 around the 1α-OH group, Y143 and S278 around the 3β-OH

group, and H305 and H397 around the 25-OH group. A pair of H-bonding residues is important for placing a hydroxyl group in its precise position within the LBP and, at the same time, for accurate folding of the LBD. In fact, the three OH groups of vitamin D derivatives in all seven of the known crystal structures[19−22] are located at exactly the same positions in the LBP. Mutational analysis showed that, in each pair of residues, one is more important than the other. Thus, for the 1α-OH group, while Ala mutation of R274 abrogated the transactivation potency, mutation of S237 to Ala had only a moderate effect. Similarly, with the 3β-OH group, Ala mutation of Y143 significantly reduced the activity but mutation of S278 to Ala elevated the potency somewhat; for the two around the 25-OH group, H397 was essential but the importance of H305 was moderate. The last example indicates that the chemical property of the residue does not determine its importance. H397 may also have a role in maintaining the stability of the active conformation, forming a π-cation-type interaction with F422 (H12), as found in LXR and FXR.[23]

Ab Initio Calculation of Hydrogen-Bonding Energies. Crystal structures that lack hydrogen atoms cannot clarify which residue acts as a hydrogen donor and which acts as an acceptor. Therefore, we tried to determine the nature of the hydrogen-bonding network around 1,25$(OH)_2D_3$ complexed with VDR by the quantum mechanical method. For this purpose, we used a novel ab initio molecular orbital (MO) method developed for proteins, the fragment molecular orbital (FMO) method.[24,25] In this method, a large protein molecule is divided into fragments, and the MOs of fragments and fragment pairs are calculated to obtain the total energy and properties of the molecule. The total electronic energy of the molecule, E_{el}, is calculated using the fragment and fragment pair energies as follows, where E_I and E_{IJ} represent the total electronic energies of fragment I and fragment pair IJ, respectively:

$$E_{el} = \sum_{I>J}^{N} E_{IJ} - (N-2)\sum_{I>J}^{N} E_I$$

We calculated the total electronic energy and interaction energies of hVDR-LBD complexed with 1,25$(OH)_2D_3$. Briefly, 3D data for hVDR-LBD/1,25$(OH)_2D_3$ (Δ165−215; PBD entry 1db1)[19] were retrieved from the PDB, the structural defect was amended, and hydrogen atoms were added automatically using the modeling software Biopolymer (Tripos). The positions of all hydrogen atoms in the molecule were refined by the molecular mechanics (MM) method (Tripos force field) for fixing heavy atoms. We carefully determined the positions of hydrogen atoms involved in hydrogen bonding between the ligand and the protein residues using model systems containing only appropriate partial structures by the ab initio MO method at the Hartree−Fock (HF) with the standard 6-31G** basis set. The coordinates of the hydrogen atoms thus determined were used to replace the original ones, which were determined by the MM method. Figure 2 shows the hydrogen-bonding profile of the ligand determined by these calculations. Using the structure thus determined, we calculated the total electronic energy of the whole hVDR-LBD/1,25$(OH)_2D_3$ complex by the FMO method at the HF/STO-3G level, where the molecule was divided into one-residue fragments and the ligand. The binding energy [$\Delta E_{interaction} = E_{complex} - (E_{receptor} + E_{ligand})$] of hVDR-LBD and 1,25$(OH)_2D_3$ was calculated to be −25.84 kcal/mol. The complex was shown to be highly stabilized by the interactions of Y143, S237, R274, H305, and H397 with the ligand, indicating the importance of these residues in formation

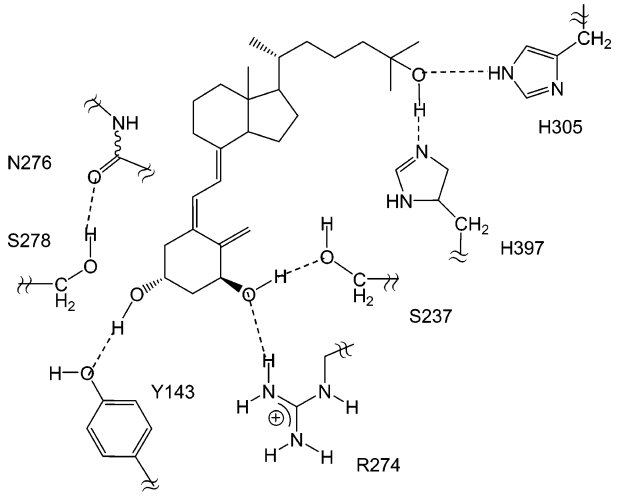

Figure 2. Hydrogen-bonding profile determined by ab initio FMO (STO-3G**)** calculation.

of the complex. Through interaction analysis between fragments, residues, and the ligand, the stabilization energies between the three OH groups and their hydrogen bond partners were evaluated to be [1α-OH, S237 (acceptor)] −5.0 kcal and [R274 (donor)] −15.6 kcal, [3β-OH group, Y143 (acceptor)] −5.2 kcal and [S278 (none)] −1.0 kcal, and [25-OH, H305 (donor)] −6.6 kcal and [H397 (acceptor)] −8.0 kcal. The total hydrogen-bonding energy of the 3β-OH group (−6.1 kcal) is smaller than those of the other two, 1α-OH (−20.5 kcal) and 25-OH (−14.7 kcal) groups, in accord with biological data. It is known that the 1α- and 25-OH groups, which are introduced by metabolic hydroxylation of vitamin D_3, have more biological importance than the 3β-OH group: removal of each of the 1α- and 25-OH groups reduces the affinity for VDR 700- and 600-fold, respectively, compared to removal of the 3β-OH group (17-fold reduction). The calculation results agree well with the ASMA data.

b. Residues 3−4 Å from the Ligand. There are 13 residues (Figure 1) within a van der Waals distance (4 Å cutoff) from the ligand. All these residues have hydrophobic interaction with the ligand. S275 may also have a proton−π interaction with the conjugated triene part. Of these, nine residues, Y147, L227, L230, L233, I271, W286, Y295, L309, and V418 are essential as Ala mutation of each nearly abolishes the activity. Each of these residues interacts not only with the ligand but also with residues on different secondary structural units, thus playing a key role in ligand-mediated protein folding. The ligand-mediated folding may have special importance to maintain the active conformation of ligand-activated NRs. NRs are known to be unstable for proteolytic cleavage when free of the ligand. Less important residues, V234, S275, C288, and V300, are less bulky or more flexible compared to the essential residues in this category. The importance of these residues changes depending on the ligand structure as described below. For example, V300 is essential for the activity of 20-epi vitamin D analogues, 20-epi-1,25$(OH)_2D_3$ (**2**) and KH1060 (**3**), but not for 22-methylated 20-epi-vitamin D, 22(*R*)-Me-20-epi-1,25$(OH)_2D_3$ (**4**).

c. Residues 4−5 Å from the Ligand. There are eight residues 4−5 Å away from the ligand (Figure 1). All essential residues in this category, F150 (loop 1−3), I268 (H4/5), L401 (H11), L404 (H11), L414 (loop 11−12), and F422 (H12), are important for protein folding: F150 in folding loop 1−3 and the latter five for folding of H12 in the active conformation. I268 (H4/5) has van der Waals contacts and/or proton−π interaction with the whole imidazole ring of H397, connecting H4/5 to H11

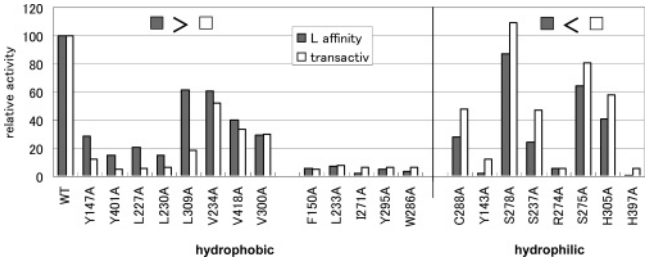

Figure 3. Ligand affinity versus transactivation. [^{3}H]1,25(OH)$_2$D$_3$ affinities of mutants (the residues within 4 Å from 1,25(OH)$_2$D$_3$): gray bars, ligand affinity; open bars, transactivation.

strongly. I268 also interacts with F422 (H12), thus stabilizing the active conformation of the VDR.

d. Residues More Than 5 Å from the Ligand. There are seven residues in this category. The two essential residues D144 and I238 are important for folding: D144 folds loop 1−3, and I238 (H3) interacts with I271 on H4/5 and L417, V421, and F422 on H12. H3 and H4/5 cross at I238 and I271 to form a loop made up of the residues of the signature region. This has a central role in forming the AF-2 surface of the LBD. Interestingly, the conformations of the pair residues I238 and I271 change simultaneously when 20-epi-1,25(OH)$_2$D$_3$ is docked in the LBP, indicating the importance of the mutual interaction. Thus, I238 is a key residue to keep, stabilizing the active conformation of the LBD, both forming a loop of signature residues and interacting intensely with the residues on H12. Among the unimportant residues, K240, E277, I314, and Q400 face both the LBP and solvent. We noticed that a group of unimportant residues (I310, L313, and I314), when lined facing the LBP, may work as an induced fit site. Recently, the X-ray crystal structure of the complex VDR-LBD/Gemini (1,25-(OH)$_2$D$_3$ derivative with the same two side chains) was reported.[26] In this complex, the second side chain of Gemini is directed to this site.

2. Effect of Mutations on the Affinity for 1,25(OH)$_2$D$_3$. We examined the effect of mutations on 1,25(OH)$_2$D$_3$ binding. We studied the ligand affinity of 19 Ala mutants that are within 4 Å from the ligand. The full-length wild-type VDR and 19 mutant VDRs were prepared in vitro in rabbit reticulocyte lysate, and their binding affinity for [^{3}H]1,25(OH) $_2$D$_3$ was determined. The results of the binding assay are shown in Figure 3 in comparison with the results of the transactivation assay. F150, L233, I271, W286, Y295, R274, and H397 were clearly essential for both ligand binding and transactivation. It is clearly evident that, for moderately important and unimportant residues, ligand binding and transcriptional activities do not parallel each other. For one group of residues, S237, Y143, S278, H305, S275, and C288, Ala mutations have larger effects on ligand binding than on transactivation, while conversely, for another group, L309, Y147, L227, L230, V234, Y401, and V418, Ala mutations have larger effects on transactivation than on ligand binding. We conclude from these results that hydrophilic residues have a greater role in ligand binding than in protein folding, and that for hydrophobic residues the opposite is true, namely, that they contribute more to protein folding than to ligand binding. Thus, as far as ligand−LBP residue interactions are concerned, hydrophobic interactions appear to be more important than hydrophilic interactions for protein shaping and, accordingly, for allosteric communication.

3. Two-Dimensional Alanine Scanning Mutational Analysis. We extended total ASMA to 2D total ASMA using 10 selected structurally characteristic ligands that included 7 agonists and 3 antagonists (Figure 4): three superagonists with

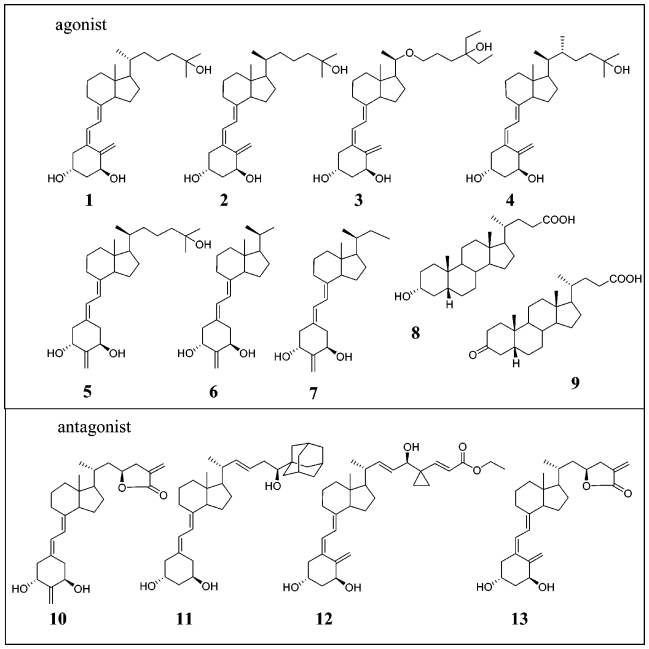

Figure 4. Structure of VDR agonists and antagonists.

a 20-epi configuration, 20-epi-1,25(OH)$_2$D$_3$ (**2**) (10^{-10} M), KH1060 (**3**) (10^{-10} M),[22] and 22(*R*)-Me-20-epi-1,25(OH)$_2$D$_3$ (**4**) (10^{-10} M);[27] two 19-nor vitamin D derivatives, 2MD (**5**) (10^{-10} M)[28] and 2MhomoP (**6**) (10^{-8} M);[20] two non vitamin D agonists, lithocholic acid (LCA, **8**) (10^{-4} M)[29] and 3-ketolithocholic acid (3-keto-LCA, **9**) (3×10^{-5} M);[29] three antagonists, LAC67 (**10**) (10^{-6} M) and AD47 (**11**) (10^{-6} M) newly developed in our laboratory and ZK168281 (**12**) (10^{-6} M) developed by Schering.[30] These compounds were subjected to the dual luciferase assay with the wild-type VDR and all 34 Ala mutant VDRs as described above. The concentration of each ligand used for this assay is the minimum concentration with which the ligand had the maximum activity.

The ASMA results for the 10 compounds are shown in Figure 5, and the overall results are summarized in a 10 × 34 patch table (Figure 6) in comparison with that of the natural hormone **1**, where the effects of mutations were categorized into three groups as described above. From the results of 2D ASMA, the following general conclusions were drawn: (1) Ten residues, Y143, D144, F150, L227, I271, R274, W286, Y295, Y401, and F422, which are essential for all agonists, are probably important for ligand-mediated folding of the LBD. (2) The activities of the other LBP mutants are ligand-sensitive, so that their behavior can offer valuable information about protein−ligand interactions. (3) The rule that mutation to a smaller Ala potentiates bulky ligands[17] holds true for antagonistic ligands, and the 2D ASMA pattern was shown to discriminate the types of antagonists.

a. 20-Epi Vitamin D$_3$ Analogues 2−4. Generally, vitamin D derivatives with the 20*S* configuration have much higher transactivation potency than the corresponding 20*R* isomers. 20-Epi-1,25(OH)$_2$D$_3$ (**2**) is accommodated in the VDR with the side chain adopting a conformation that is significantly different from that of the natural hormone **1**, although it adopts nearly the same conformation at other parts. Also when complexed with 20-epi vitamin D compounds **2** and **3**, the conformations of the LBP residues change at two residues, I238 and I271, as described above.[19,22] Apparently, the conformational changes of I238 and I271 are linked. Different interactions of compound **2** with the LBP residues in comparison with those of **1** appear in the 2D ASMA: V300 is essential for its potency, in addition to the 20 residues important for the natural hormone **1**. We

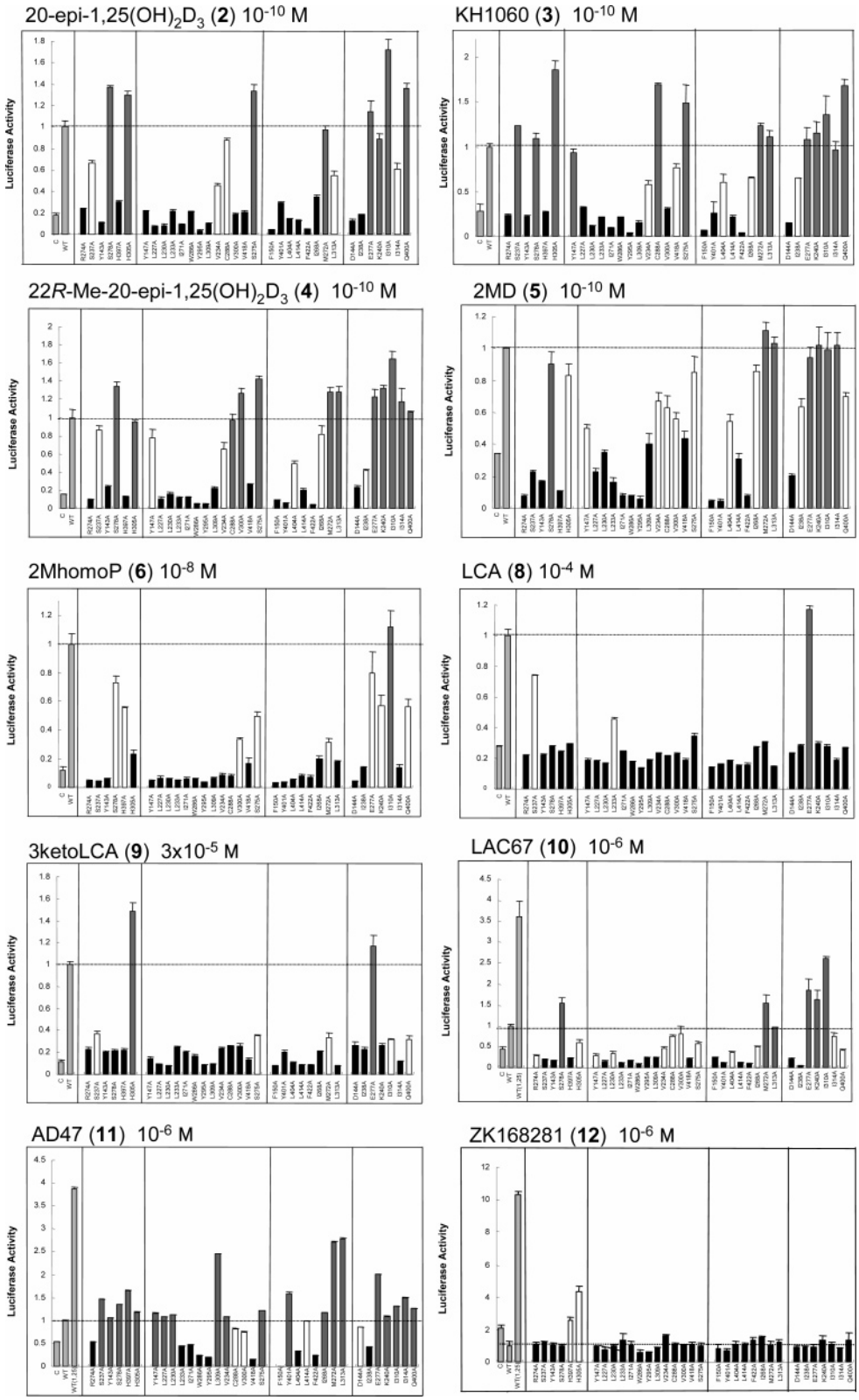

Figure 5. 2D ASMA results of seven synthetic agonists and three antagonists. The activities were evaluated by dual luciferase assay using a wild-type or mutant full-length hVDR expression plasmid (pCMX-hVDR) and a luciferase reporter gene with a mouse osteopontin VDRE at the promoter (SPPx3-TK-Luc) in COS7 cells. Concentration of the ligands: 20-epi-1,25(OH)$_2$D$_3$ (**2**) (10^{-10} M), KH1060 (**3**) (10^{-10} M), 22(*R*)-Me-20-epi-1,25(OH)$_2$D$_3$ (**4**) (10^{-10} M); 2MD (**5**) (10^{-10} M), 2MhomoP (**6**) (10^{-8} M), LCA (**8**) (10^{-4} M), 3-keto-LCA (**9**) (3×10^{-5} M), LAC67 (**10**) (10^{-6} M), AD47 (**11**) (10^{-6} M), and ZK168281 (**12**) (10^{-6} M). Effects of mutation on the transactivation are discriminated by colors: black, mutation significantly reduced (<20% for agonists) the activity of the wild-type VDR; white, mutation had a moderate effect (20−90%); gray, mutation had little effect or even elevated the potency (>90%).

assumed that this residue plays a role in the superagonistic activity of **2**. V300 is essential for not only 20-epi-1,25(OH)$_2$D$_3$ (**2**) but also KH1060 (**3**), but not for the 22*R*-methylated analogue (**4**), indicating the importance of the interaction at C(22) with V300 for the action of 20-epi vitamin D compounds. From the 2D ASMA data, we assume that the hydrophobic

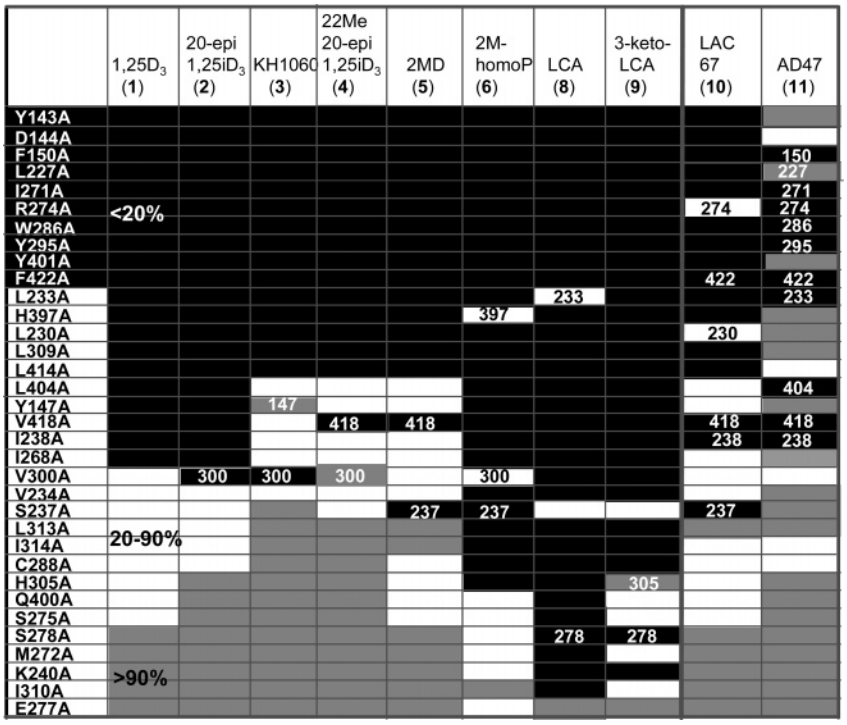

Figure 6. Patch table presentation of 2D ASMA for 11 VDR ligands. Effects of mutation on the transactivation are discriminated by colors: black, mutation significantly reduced (<20% for agonists) the activity of the wild-type VDR (WT); white, mutation had a moderate effect (20−90%); gray, mutation had little effect or even elevated the potency (>90%). The percentage effects were corrected for the background activity (C) of endogenous VDR in COS7 cells.

network made from V300 (H6)−C(22)-ligand-C(19)−I271 (H4/5)−I238 (H3)−L417, V421, and F422 (H12) would stabilize the active conformation of the VDR-LBD as described below (Figure 9D). Ala mutations of H305 and S275 rather enhance the potency of 20-epi-1,25$(OH)_2D_3$, suggesting that these residues are sterically repelled from the ligand. For KH1060 (**3**), L404, V418, I238, and I268 have only moderate importance, probably because its bulky side chain contributes to stabilization of the active conformation in the region around these residues. We have reported that the number of Ala mutations that enhance the potency increases with increasing ligand volume. The potency of KH1060 is enhanced by mutations at 11 residues: E277, S278, L313, K240, S237 M272, I310, S275, C288, Q400, and H305. We suggest that increased ligand volume reinforces the van der Waals contacts with LBP residues, but at the same time also increases the steric stress in the complex; consequently, the Ala mutations would release these steric stresses. Furthermore, residues for which Ala mutation enhances the potency are not restricted to the area around the bulky portion of the ligand, but are distributed all around the ligand. In the case of KH1060, steric congestion at the side chain terminal affects the residues in the distant position in the LBP, such as S237, S275, C288, M272, and I310. H305A has higher activity (130−180%) than wtVDR when 20-epi-1,25$(OH)_2D_3$ (**2**) or KH1060 (**3**) is accommodated. Relief of the steric strain between H305 and the side chain part of the ligand may be the reason for this potentiation.

b. 19-Nor vitamin D analogues show some characteristics. 2MD (**5**) is an analogue in which the 10,19-exocyclic methylene of natural vitamin D is displaced by the C(2) methylene and has unexpectedly high potency: compared with the natural hormone, it has 4 times the VDR affinity and 100 times the transactivation. This compound is also reported to have bone-selective action.[28] The crystal structure of 2MD (**5**) complexed with rat VDR has been reported.[20] The three hydroxyl groups of 2MD (**5**) occupy exactly the same positions in the LBD as those of the natural hormone **1**. However, the CD ring and the side chain parts of 2MD (**5**) adopt conformations significantly different from those of **1**. The fact that the important residue F150 is within a van der Waals contact region from the methylene at C(2) would be the reason for its high potency. In comparison with 20-epi-1,25$(OH)_2D_3$ (**2**), 2MD (**5**) requires less essential residues for its proper action. The higher the potency, fewer essential residues the ligand requires. The key residue for the function of 2MD (**5**) may be S237. Loss of the 10(19)-methylene may strengthen the hydrogen bond between S237 and the 1α-OH group and, in turn, the interaction between H3 and H4/5, which would have a beneficial effect on the formation of the AF-2 surface and dimer interface.

2MhomoP (**6**) has about 10% VDR affinity and transcriptional activity similar to that of the natural hormone, despite loss of the 25-hydroxyl group of generally active vitamin D compounds. 2MhomoP (**6**) probably uses a water molecule incorporated into the LBP, making the transcriptionally active form stable and forming a hydrogen bond with H305 and H397, as is the case in the analogous 2MbisP (**7**). 2MbisP (**7**) is a one methylene longer homologue of 2MhomoP (**6**), and recently, analysis of its crystal structure when complexed with rVDR (PDB entry 1rkg)[20] showed that a water molecule is incorporated in the H11 site of the LBP: its oxygen occupies exactly the same position as O(25) of 1,25$(OH)_2D_3$ (PDB entry 1db1), and furthermore, the water oxygen forms hydrogen bonds with H305 and H397.

2MhomoP (**6**) shows a 2D ASMA pattern significantly different from that of the natural hormone: 25 residues are essential to retain its potency.

c. LCA compounds 8 and 9 have significantly lower activity than the active vitamin D compound: their transcriptional activities are 3000−10000 times weaker than that of 1,25-$(OH)_2D_3$. LCA compounds have two hydrophilic groups at the two terminals (COOH at one end and C═O or OH at the other) but lack the OH group corresponding to the 1α-OH group of active vitamin D compounds that tightly connects H3 and H4/

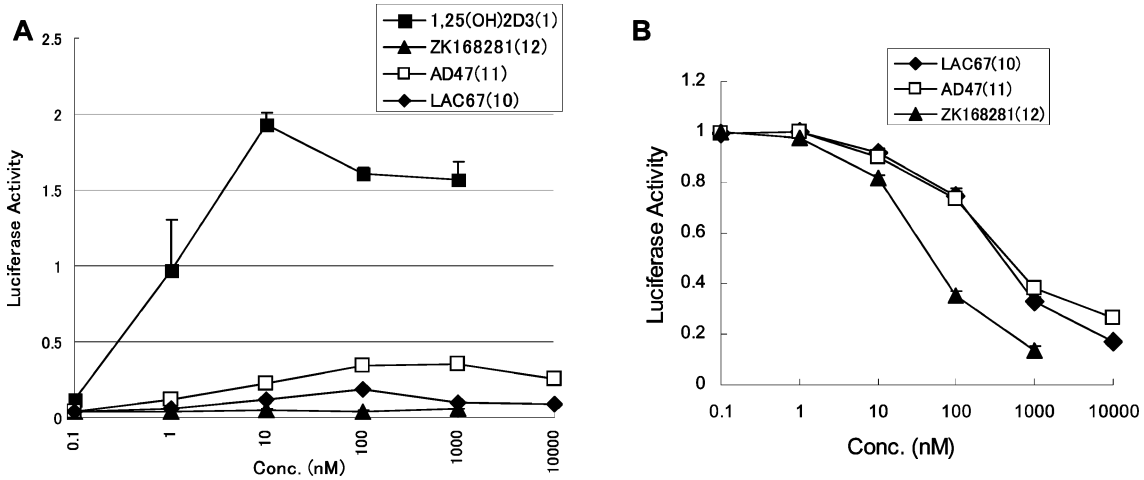

Figure 7. Activities of new antagonists AD47 (**11**) and LAC67 (**10**). The transcriptional activity (A) and inhibitory effect on the transactivation induced by $1,25(OH)_2D_3$ (B) were evaluated in comparison with ZK16281 (**12**) by dual luciferase assay using a wild-type full-length hVDR expression plasmid (pCMX-hVDR) and a luciferase reporter gene with a mouse osteopontin VDRE at the promoter (SPPx3-TK-Luc) in COS7 cells. In the antagonist activity test, the cells were treated with 10^{-8} M $1,25(OH)_2D_3$ in the presence or absence of indicated concentrations of antagonists.

5. This explains its low affinity for the VDR and low transcriptional activity. Instead, Ser278 is essential for anchoring LCAs in the LBP: Ser278 has little importance for active vitamin D compounds. Most LBP residues are required for the activity, because of the inefficient interaction with the LBP residues shown by these compounds. It is noteworthy that LCA and 3-keto-LCA show distinct patterns. This is the reason we suggested two different docking modes for these two compounds, as reported previously:[17] the side chain carboxyl group is directed toward H12 in the LCA model, while the carboxyl group is oriented toward the β-turn in the 3-keto-LCA model.

d. VDR Antagonist. Crystal structures of NRs complexed with antagonistic ligands have been reported,[9,10,31] and these data have helped to clarify the mechanism of action of the antagonists. NR ligands that bind strongly but prevent the LBD from adopting the active conformation function as receptor antagonists. A group of NR antagonists, such as hydroxyl tamoxifen[31] and raloxifene,[9] have a bulky structural unit that creates spatial restriction with residues on H12 in the active conformation. When these ligands bind to the cognate receptor, H12 is prevented from occupying the right position on the AF-2 surface and transactivation of the target genes is inhibited, because coactivators cannot be recruited to the surface of the NR. We term this type of antagonist type I. The other group of antagonists have no such bulky structural unit, which might prevent the core part of the NR from adopting the active conformation, and thus prevent the correct positioning of H12. For example, progesterone works as an antagonist of the mineral corticoid receptor (MR) because, with this ligand, MR has insufficient interaction between H3 and H4/5.[32] It is also reported that exact positioning of H11 is important for H12 to adopt the active conformation in ERβ.[14,15] We term this second group of antagonists type II. In the case of the VDR, two such antagonist types are also known: ZK compounds (such as ZK168281, **12**) developed by the Schering group[30] are clearly type I antagonists, since they have a long ester group at the side chain terminal that causes spatial restriction with H12 in the active conformation; TEI compounds (such as TEI9647, **13**) developed by the Teijin group,[33,34] which have a methylene lactone structure in the side chain, can be categorized as type II because they have no bulky structure directed toward H12. We were able to discriminate these two types of VDR antagonists by 2D ASMA.

For 2D ASMA we used three antagonists, AD47 (**11**) and LAC67 (**10**) (newly synthesized by our group, unpublished results) and ZK16281 (**12**) (Figure 4). We designed AD47 (**11**) as a type I antagonist that has a bulky adamantane ring at the side chain terminal and LAC67 (**10**) as a TEI compound analogue. Our two compounds (**10** and **11**) were evaluated for the VDR affinity, transactivation potency, and inhibitory effect on the transactivation induced by $1,25(OH)_2D_3$ in comparison with ZK16281 (**12**). AD47 (**11**) and LAC67 (**10**) were found to have moderate affinity for the VDR, being 1/50 and 1/10 that of the natural hormone, respectively. AD47 and LAC67 have weak transcriptional activity (Figure 7A). Both AD47 (**11**) and LAC67 (**10**) inhibited the transactivation induced by $1,25-(OH)_2D_3$ dose-dependently with an IC_{50} of 4×10^{-7} and 3×10^{-7} M, respectively (Figure 7B). The antagonistic activities of these compounds were 1/8 to 1/6 that of ZK16281 (**11**) ($IC_{50} = 5 \times 10^{-8}$ M).

2D ASMA of Antagonists. We subjected the three antagonists ZK16281 (**12**; 10^{-6} M), AD47 (**11**; 10^{-6} M), and LAC67 (**10**; 10^{-6} M) to 2D ASMA, and the results are shown in Figures 5 and 6. With the ZK compound **12**, Ala mutations of most (21) residues had little effect on the transcriptional activity, as it has full antagonistic activity (Figure 5). Interestingly, mutations of H305 and H397 resulted in 4.3- and 2.6-fold recovery of the activity, respectively. The 24-OH group of ZK **12** probably forms hydrogen bonds with these two His residues in a manner similar to that of the analogous MC903 for which the crystal structure when complexed with the VDR (PDB entry 1s19) has been reported.[21] These hydrogen bonds are expected to fix the side chain of the ZK compound, so that the bulky ester group is forced to push H12 out. Mutation of either His to Ala reduces the hydrogen-bonding ability, increases the flexibility of the side chain of **12**, and in addition yields room for the side chain of **12** to be packed in.

Two antagonists, LAC67 **(10)** and AD47 **(11)**, showed distinct 2D ASMA patterns (Figure 6). AD47 (**11**) showed a patch table pattern similar to those of agonists with a bulky side chain, such as KH1060 (**3**) and 22(*R*)-Me-$1,25(OH)_2D_3$ (**4**): Ala mutations elevate potency with the number of residues around the ligand, as described above. In the case of AD47 (**11**), Ala mutation

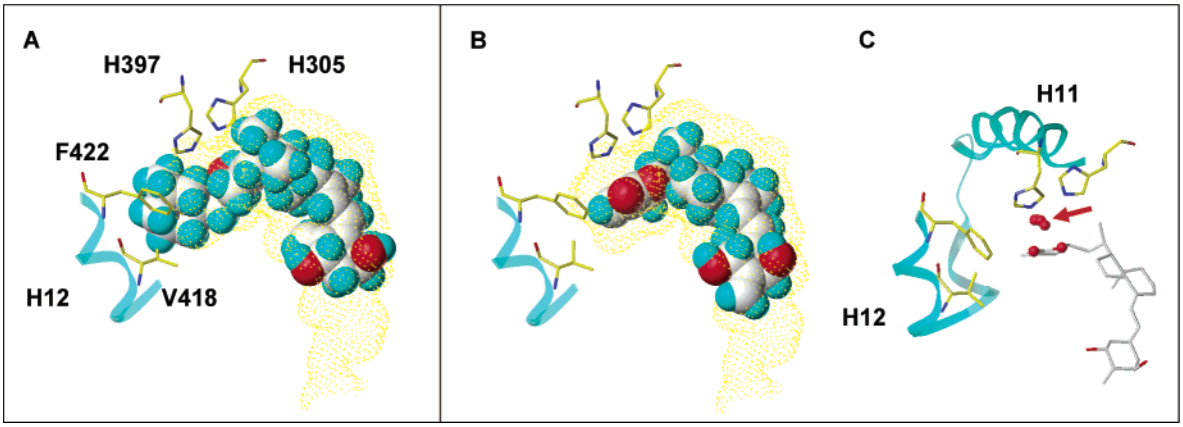

Figure 8. Docking models of AD47 and Lac67 in VDR-LBP: (A) AD47 (space fill, atom type and color) in the VDR-LBP (Connolly channel surface, yellow dot) with interacting residues (stick, yellow carbon); (B) Lac67 (space fill, atom type and color) in VDR-LBP; (C) Lac67 (stick, atom type and color) with interacting residues (stick, yellow carbon). The red arrow shows the positions of the side chain oxygens (24-, 25-, or 26-OH) of seven agonists complexed with VDR-LBD (N. Rochel et al., 2000; G. Tocchini-Valentini et al., 2001; J. L. Vanhooke et al., 2004; G. Tocchini-Valentini et al., 2004). H12 and H11 are shown with ribbon loop rendering.

has little effect or elevates the potency at 21 residues. However, mutations of F150, L233, I238, I271, W286, Y295, V418, L404, and F422 still reduced the transcriptional activity significantly. The fact that I238, I271, L404, V418, and F422 are important for transactivation indicates that AD47 (**11**) activates the VDR by forming an active conformation, although its adamantane part creates spatial restriction with H12 in the active conformation, as the model structure shows (Figure 8A).

LAC67 (**10**) shows a pattern distinct from those of type I antagonists in the patch table but rather similar to those of normal agonists (Figure 6), even though this compound has antagonistic activity similar to that of AD47 (**11**). Thus, 2D ASMA demonstrated clear differences between type I and type II antagonists, suggesting a difference in the mechanisms of antagonistic action between the two. How do methylene lactone type antagonists work? The methylene lactone LAC67 probably forms a hydrogen bond with H397 or H305, since it has high VDR affinity (1/10). Docking analysis suggests that H397 may be the hydrogen bond partner (Figure 8B,C). However, as the docking model shows, the carbonyl oxygen of the lactone occupies a position distinct from that of the 25-oxygen of the natural hormone in its VDR complex. In the crystal structures of all eight VDR/ligand complexes, the 25-oxygen and its equivalents occupy exactly the same place between H305 and H397 (Figure 8C).[19−22] When complexed with methylene lactone compounds, H397 would shift its position to form a hydrogen bond with the lactone carbonyl, and this would shift, in turn, the position of H11. We speculate that the hydrogen bond between H397 and the ligand (including a water molecule incorporated in the LBP) is crucial for accurate positioning of H11 and that methylene lactone compounds show antagonistic activity because of the lack of a hydroxyl group corresponding to the 25-oxygen of the natural hormone. 2D ASMA of LAC67 (**10**) indicated that F422, V418, and I238 are essential for the transactivation of this compound. This indicates that ligand-mediated folding of H12 in the active conformation is still working when LAC67 elicits transactivation potency: V418 (H12) probably has van der Waals contact with the methylene group on the lactone ring. LAC67 (**10**) also shows a pattern similar to that of 2MD-type compounds at L230, L404, L147, and S237.

4. Ligand-Mediated Allosteric Network. How are the allosteric effects imprinted by ligands transmitted to the interfaces where the NR interacts with the dimer partner and transcriptional coactivators? Schulman et al., using the SCA approach, found an evolutionally conserved network.[12] However, the phylogenetic approach cannot clarify the contribution of LBP residues to the allosteric network, since the residues forming the LBP have been evolutionally selected to achieve ligand specificity. In fact, none of the 36 LBP residues of hVDR are among the network residues selected by SCA (Figure 9A). The SCA network residues are found mainly in the signature region and the core part that is essential for maintaining the 3D structure of NR-LBD. We were able to know the functions of all the LBP residues from the total 2D ASMA study: the functions of 20 essential residues are summarized in Table 1. On the basis of these data, we suggest the following ligand-mediated allosteric networks of the VDR (Figure 9B−E).

a. Network Linked to the AF-2 Surface and Dimer Interface (Figure 9B,C). By means of this network, the effects of ligands might be transmitted to the AF-2 surface and dimer interface. H3 and H4/5 are tightly connected directly at I238 and V234 on H3 and at I271 on H4/5, and via the ligand (1α-OH) at S237 (H3) and R274 (H4/5), to form a loop comprising the residues of the signature region[5] which forms the most important surface of the LBD for the transactivation function (static AF-2 surface). It should be noted that 9 (F244, A245, K246, P249, F251, D258, Q259, L262, and L263) out of the 15 signature residues are involved in the SCA network suggested by Shulman et al.: the SCA residues are shown with blue balls in Figure 9B−E. As H3 and H4/5 are tightly bound, the residues on loop 11−12 become interactive with the residue on H3 and move up along H3, finally becoming bent at P416 to form H12. The residues on H12, L417, and F422 are then fixed by binding to the residues on H3 (I238) and H11 (H397 and Y401), respectively, to complete the AF-2 surface. The ligand has a van der Waals contact at C-26 with V418 on H12 to stabilize the active conformation from inside. We should note that this network also links at H4/5 and H12 to the residues of the SCA network (italic): I271 (H4/5)−*E269* (H4/5)−*L390* (H10/11)−*R391* (H10/11)−*D342* (H8) (Figure 9C) and I238 (H3)−*L417* (H12) (Figure 9B). Thus, we were able to identify the network that transmits the effect of the ligands to the dimer interface (H10/11) and the AF-2 surface. A mutation (R391C) of the residue, which is involved in this network and is exposed on the dimer interface, is known to cause severe rickets accompanied by alopecia.[35] These authors also reported that the transactivation potency of R391C was effectively restored by boosting the level of either RXR or $1,25(OH)_2D_3$. Interestingly, however, point mutants R391C and R391A had transcriptional

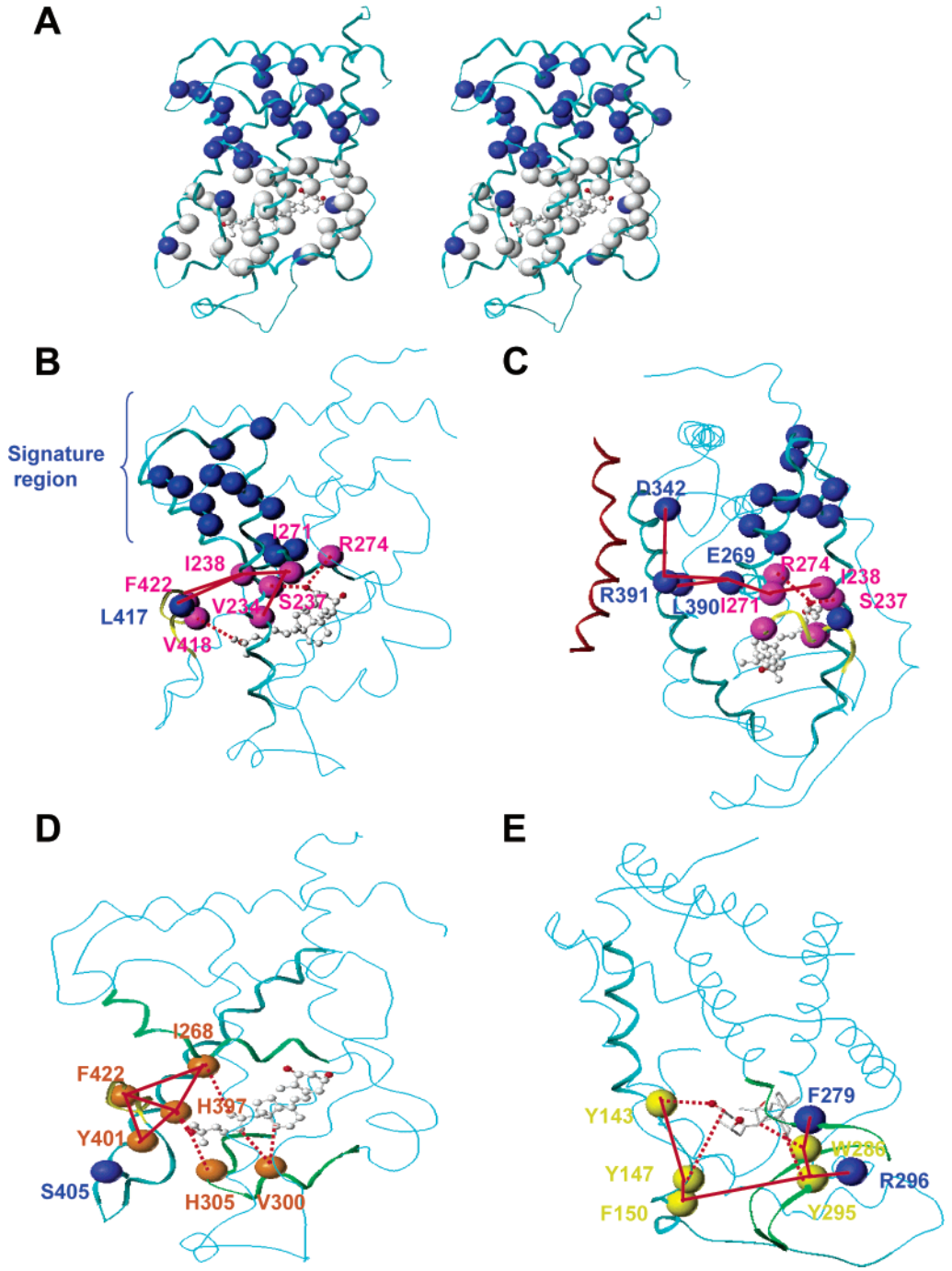

Figure 9. Allosteric network of VDR. (A) Allosteric network residues determined by SCA (blue balls) and the residues lining the LBP (white balls) (stereoview). (B, C) Ligand-mediated allosteric network that transmits the effects of the ligand to the AF-2 surface (B) and the dimer interface (C). The residues involved in this network are shown with magenta balls at Cα. SCA residues are shown with blue balls. H3 and H12 are shown with cyan and yellow ribbon renderings, respectively, and other parts of the LBD are shown with cyan wire. Interactions between amino acid residues and the ligand are shown with red dotted lines and those between residues with red lines. The red ribbon in panel C shows H10/11 of the dimer partner RXR in a VDR−RXR heterodimer model. (D) Ligand-mediated allosteric network that is important for positioning of H11. The residues involved in this network are shown with orange balls at Cα. H4/5, H11, H6−H7, and H12 are shown with blue-green, cyan, green, and yellow ribbon loop renderings, respectively, and other parts of the LBD are shown with cyan wire. This model is drawn using the hVDR-LBD/20-epi-1,25$(OH)_2D_3$ (**2**) complex (PDB entry 1ie9). (E) Ligand-mediated allosteric network that forms a wall of aromatic residues at the β-turn side: the residues involved in this network are shown with yellow balls at Cα. H1 to loop 1−3 and β-strands are shown with cyan and green ribbon loop renderings, respectively, and other parts of the LBD are shown with cyan wire.

potencies similar to those of wtVDR in our in vitro transient transcription assay system when activated by 1,25$(OH)_2D_3$ (**1**) (Figure 10). The effects of seven ligands (**2**−**6**, **8**, and **9**) on the activity of R391A and R391C were also examined, and the results are shown in Figure 10. By these mutations (R391A and R391C), the transcriptional activities of highly active compounds **2**, **3**, and **5** were found to be little affected, but those of 2MhomoP (**6**), LCA (**8**), and 3-keto-LCA (**9**) were reduced significantly to 40%, 40%, and 25% that of wtVDR, respectively. It should be noted that these mutations elevate the potency of 22(*R*)-Me-1,25$(OH)_2D_3$ (**4**), which has the highest VDR affinity (10-fold that of **1**) of all vitamin D compounds known.[27] These results with 1,25$(OH)_2D_3$ (**1**) and LCA (**8**) are in good agreement with those reported by Schulman et al. (2004),[12] who

Table 1. Essential Residues Lining the LBP of VDR and Their Predicted Functions

residue	position	major function
		Ten Essential Residues for all VDR Agonists Activating VDR
Y143	H1	ligand-mediated folding of the β-turn side
D144	L1−3	folding of the β-turn side
F150	L1−3	ligand-mediated folding of the β-turn side
L227	H3	folding of the AF-2 surface
I271	H4/5	binding of H3 and H4/5 and folding of the active conformation
R274	H4/5	ligand-mediated packing of H3 and H4/5 and folding of the active conformation
W286	β-turn	ligand-mediated folding of the β-turn side
Y295	β-turn	ligand-mediated folding of the β-turn side
Y401	H11	binding of H11 and H12 and folding of the AF-2 surface
F422	H12	packing of H12 against H3, H4/5, and H11 and folding of the AF-2 surface
		Ten Additional Essential residues for 1,25(OH)$_2$D$_3$ Activating VDR
L233	H3	ligand folding and connection of H3 to the β-turn side
H397	H11	positioning of H11 and folding of the active conformation
L230	H3	connection of H3 to the β-turn side
L309	H7	folding of the dimer interface
L414	L11−12	folding of the AF-2 surface
L404	H11	folding of the AF-2 surface
Y147	L1−3	ligand-mediated folding of the β-turn side
V418	H12	ligand-mediated folding of the AF-2 surface
*I*238	H3	connection of H3 and H4/5 and folding of the active conformation
I268	H4/5	positioning of H11

explained that the allosteric network predicted by SCA is required for mediating metabolic signaling such as for LCA, but not for endocrine ligands such as 1,25(OH)$_2$D$_3$. We assume that the mutations R391A and R391C had a significant effect on the potency of LCA, because LCA is unable to mediate the interaction of H3 with H4/5, since it has no OH group corresponding to the 1α-OH of active vitamin D compounds. Therefore, the allosteric effect of this ligand cannot be efficiently transmitted to the network.

b. Network for Positioning of H11 (Figure 9D). Positioning of H11 is important for forming the active conformation.[14,15] We found a network that is important for positioning of H11 in the VDR-LBD. This network connecting H6 (V300) and loop 6−7 (H305) to H11 (H397) via the ligand, C(12) and 25-OH, bottoms up the LBP at H6 to the loop 6−7 part and further links to the residue (F422) on H12. H397 at H11 also has tight contacts with I268 at H4/5, which interacts with F422 at H12 and the ligand [C(22) of 1,25(OH)$_2$D$_3$ (**1**) and C(21) of 20-epi-1,25(OH)$_2$D$_3$ (**2**)]. This network is strengthened in 20-epi vitamin D analogues by adding new interactions: H6 (V300)−ligand C(22) and loop 6−7 (H305)−ligand C(23)−H11 (H397). H11 ends up with an SCA residue, S405, that may act as the helix-breaking residue.

c. Blocking of Aromatic Residues at the β-Turn Side (Figure 9E). There is a group of important aromatic residues, Y143, Y147, F150, W286, and Y295, at the β-turn side. These residues are connected to F279 and R296 of SCA residues and form a wall at the β-turn side of the LBP. The function of this part of the LBD is not known, but these residues appear to stabilize this fragile region containing many loop structures.

NR ligands including steroid hormones, vitamin D, thyroid hormones, and retinoids have proved to be clinically essential drugs. Since the clarification of the 3D structures of NR/ligand complexes, NRs have again attracted much attention as targets for NR structure-based drug design. In the present study using exhaustive ASMA of the hVDR-LBP, we have provided basic data for understanding the interactions of NR ligands and the residues directly facing the ligand and their effects on the transactivation potency. We identified the LBP residues that play a key role in transactivation function and the ligand-mediated allosteric network that transmits the effects of the ligand to dimer and coactivator interfaces. 2D total ASMA was shown to compensate for the defects of the SCA approach. In fact, the ligand-mediated allosteric network was shown to be connected to the network suggested by SCA, thus completing the whole network by which information from a ligand is transmitted to the interfaces between protein cofactors. Since the structure−function relationship is basically common among the NR family, our findings will be applicable to other NR family members.

Experimental Procedures

Graphical Manipulations and Ligand Docking. Graphical manipulations were performed using SYBYL 6.9 (Tripos, St. Louis). The atomic coordinates of the crystal structure of hVDR-LBD (Δ165−215) were retrieved from the PDB (entry 1db1). Vitamin D analogues were docked into the ligand-binding pocket manually or using the docking software FlexX (version 1.11.0).

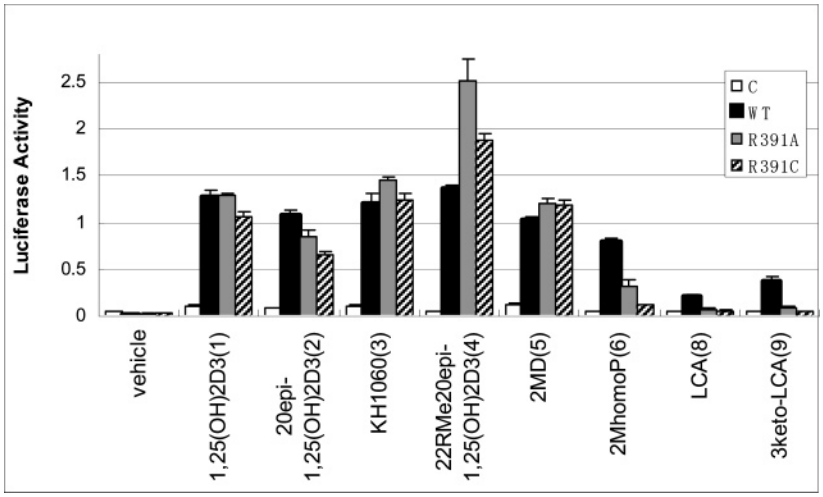

Figure 10. Transcriptional activities of R391A and R391C induced by various ligands. The activities were evaluated by dual luciferase assay using a wild-type or mutant (R391A or R391C) full-length hVDR expression plasmid (pCMX-hVDR) and a luciferase reporter gene with a mouse osteopontin VDRE at the promoter (SPPx3-TK-Luc) in COS7 cells. Concentration of the ligands: 20-epi-1,25(OH)$_2$D$_3$ (**2**) (10^{-10} M), KH1060 (**3**) (10^{-10} M), 22(*R*)-Me-20-epi-1,25(OH)$_2$D$_3$ (**4**) (10^{-10} M), 2MD (**5**) (10^{-10} M), 2MhomoP (**6**) (10^{-8} M), LCA (**8**) (10^{-4} M), and 3-keto-LCA (**9**) (3×10^{-5} M).

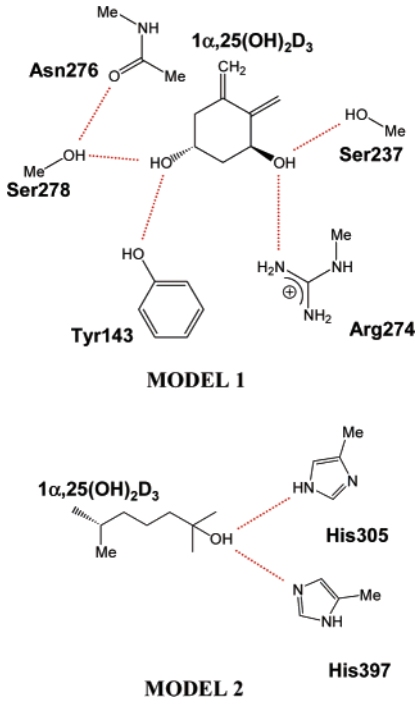

Figure 11. Model systems used to determine the positions of the active hydrogen atoms involved in the hydrogen bond network around the three hydroxyl groups of $1,25(OH)_2D_3$.

Site-Directed Mutagenesis. The hVDR expression vector pCMX-hVDR[36] was used as a template for in vitro site-directed mutagenesis. Point mutants were created using a Quick-Change Site-Directed Mutagenesis Kit (Stratagene, CA). Using synthetic oligonucleotides, 34 clones of mutated hVDRs from pCMX-hVDR were produced as described by the manufacturer. *Escherichia coli* DH5α competent cells were transformed with the vectors incorporating the desired mutations. The cDNAs of the clones were purified by a Qiafilter Plasmid Maxi-Kit (Qiagen, Valencia, CA), and the presence of the desired mutation was confirmed by DNA sequencing.

Transfection and Transactivation Assay. COS-7 cells were cultured in Dulbecco's modified Eagle's medium (DMEM) supplemented with 5% fetal calf serum (FCS). Cells were seeded on 24-well plates at a density of 2×10^4 per well. After 24 h, the cells were transfected with a reporter plasmid containing three copies of the mouse osteopontin VDRE (5′-GGTTCAcgaGGTTCA, SPPx3-TK-Luc), a wild-type or mutant hVDR expression plasmid (pCMX-hVDR), and the internal control plasmid containing sea pansy luciferase expression constructs (pRL-CMV) by the lipofection method as described previously.[17,18] After 4 h of incubation, the medium was replaced with fresh DMEM containing 5% charcoal-treated FCS (HyClone, Utah). The next day, the cells were treated with either the ligand or ethanol vehicle and cultured for 24 h. Cells in each well were harvested with a cell lysis buffer, and the luciferase activity was measured with a luciferase assay kit (Toyo Ink, Inc., Japan). Transactivation measured by the luciferase activity was normalized with the internal control. All experiments were done in triplicate. In the antagonist activity test, the cells transfected as described above were treated with 10^{-8} M $1,25(OH)_2D_3$ in the presence or absence of indicated concentrations of antagonists.

Cell-Free Transcription and Translation. Plasmids (1 μg) containing the cDNA coding for the wild-type hVDR or for mutant hVDRs were expressed in vitro using the T7-coupled rabbit reticulocyte lysate system (Promega, Madison, WI) according to the manufacturer's instructions.

Ligand-Binding Assay. After translation of the wild-type hVDR or the mutant hVDRs, the lysate was diluted 5-fold with ice-cold TEGWD buffer (20 mM Tris−HCl, pH 7.4, 1 mM EDTA, 1 mM dithiothreitol, 20 mM sodium tungstate, and 10% glycerol). The diluted lysate was incubated with an increasing concentration of $1,25(OH)_2[26,27\text{-}methyl\text{-}^3H]D_3$ (0.056−2.78 nM) for 16 h at 4 °C in the presence or absence of a 400-fold molar excess of unlabeled $1,25(OH)_2D_3$. Bound and unbound ligands were separated by the dextran−charcoal method. Bound ligand was quantitated using scintillation counting.

FMO Calculation. The MOs and total electronic energies of the hVDR-LBD (Δ165−215)/$1,25(OH)_2D_3$ complex and its components were calculated by the following procedures. (1) 3D data of the hVDR-LBD (Δ165−215)/$1,25(OH)_2D_3$ complex (1db1) were retrieved from the PDB, and its structural defects were amended: (i) the missing loop 8−9 (375−377) was amended by using the data of the same part in the crystal structure of the hVDR-LBD Δ165−215/20-epi-$1,25(OH)_2D_3$ complex (1ie9) and by using the software Biopolymer (Tripos); (ii) hydrogen atoms were added automatically using Biopolymer; (iii) N- and C-terminals were amended to NH_2 and COOH, respectively. (2) The positions of automatically added hydrogen atoms in the amended VDR-LBD were refined by the energy minimization using the molecular mechanics routine of Sybyl (Tripos force field, Powell method). (3) The positions of the active hydrogen atoms involved in the hydrogen bond network around the three hydroxyl groups of $1,25(OH)_2D_3$ were optimized using model systems (Figure 11, models 1 and 2) by the ab initio MO calculation at the HF/6-31G** level. (4) The coordinates of the hydrogen atoms in the hydrogen bond network thus calculated were used to replace the original ones, which were determined by the MM method in step 2, to give the structure of the VDR-LBD/$1,25(OH)_2D_3$ complex for ab initio FMO calculation. The structural data for apo-VDR-LBD and the ligand $1,25(OH)_2D_3$ were made by eliminating the coordinates of the ligand and the protein, respectively. (5) We calculated the MOs and total electronic energies of the VDR-LBD/$1,25(OH)_2D_3$ complex and its components, the protein and the ligand, using the structures obtained in step 4 by the ab initio FMO method at the HF/STO-3G level. In these FMO calculations, the protein was divided into one-residue fragments cutting at the Cα of each residue and the ligand $1,25(OH)_2D_3$ was treated as a fragment. All FMO calculations were performed by using the ABINIT-MP program (available from http://www.fsis.iis.u-tokyo.ac.jp/en/resutls/software/).

Acknowledgment. The calculation part of this research was supported by CREST, JST.

References

(1) Evans, R. M. The steroid and thyroid hormone receptor superfamily. *Science* **1988**, *240*, 889.
(2) Mangelsdorf, D. J.; Thummel, C.; Beato, M.; Herrlich, P.; Schutz, G.; Umesono, K.; Blumberg, B.; Kastner, P.; Mark, M.; Chambon, P.; Evans, R. M. The nuclear receptor superfamily: the second decade. *Cell* **1995**, *83*, 835−839.
(3) Perissi, V.; Staszewski, L. M.; McInerney, E. M.; Kurokawa, R.; Krones, A.; Rose, D. W.; Lambert, M. H.; Milburn, M. V.; Glass, C. K.; Rosenfeld, M. G. Molecular determinants of nuclear receptor-corepressor interaction. *Genes Dev.* **1999**, *13*, 3198−3208.
(4) Darimont, B. D.; Wagner, R. L.; Apriletti, J. W.; Stallcup, M. R.; Kushner, P. J.; Baxter, J. D.; Fletterick, R. J.; Yamamoto, K. R. Structure and specificity of nuclear receptor-coactivator interactions. *Genes Dev.* **1998**, *12*, 3343−3356.
(5) Wurtz, J. M.; Bourguet, W.; Renaud, J. P.; Vivat, V.; Chambon, P.; Moras, D.; Gronemeyer, H. A canonical structure for the ligand-binding domain of nuclear receptors. *Nat. Struct. Biol.* **1996**, *3*, 87−94.
(6) Bourguet, W.; Ruff, M.; Chambon, P.; Gronemeyer, H.; Moras, D. Crystal structure of the ligand-binding domain of the human nuclear receptor RXR-α. *Nature* **1995**, *375*, 377−382.
(7) Renaud, J.-P.; Rochel, N.; Ruff, M.; Vivat, V.; Chambon, P.; Gronemeyer, H.; Moras, D. Crystal structure of the RAR-γ ligand-binding domain bound to all-*trans* retinoic acid. *Nature* **1995**, *378*, 681−689.
(8) Egea, P. F.; Mitschler, A.; Rochel, N.; Ruff, M.; Chambon, P.; Moras, D. Crystal structure of the human RXRα ligand-binding domain bound to its natural ligand: 9-*cis* retinoic acid. *EMBO J.* **2000**, *19*, 2592−2601.

(9) Brzozowski, A. M.; Pike, A. C.; Dauter, Z.; Hubbard, R.; Bonn, T.; Engstrom, O.; Ohman, L.; Greene, G. L.; Gustafsson, J. A.; Carlquist, M. Molecular basis of agonism and antagonism in the oestrogen receptor. *Nature* **1997**, *389*, 753−758.
(10) Xu, H. E.; Stanley, T. B.; Montana, V. G.; Lambert, M. H.; Shearer, B. G.; Cobb, J. E.; McKee, D. D.; Galardi, C. M.; Plunket, K. D.; Nolte, T.; Parks, D. J.; Moore, J. T.; Kliewer, S. A.; Willson, T. M.; Stimmel, J. B. Structural basis for antagonist-mediated recruitment of nuclear co-repressors by PPARα. *Nature* **2002**, *415*, 813−817.
(11) Peleg, S.; Liu, Y. Y.; Reddy, S.; Horst, R. L.; White, M. C.; Posner, G. H. A 20-epi side chain restores growth-regulatory and transcriptional activities of an A ring-modified hybrid analog of 1α,25-dihydroxyvitamin D_3 without increasing its affinity to the vitamin D receptor. *J. Cell. Biochem.* **1996**, *63*, 149−161.
(12) Shulman, A. I.; Larson, C.; Mangelsdorf, D. J.; Ranganathan, R. Structural Determinants of Allosteric Ligand Activation in RXR Heterodimers. *Cell* **2004**, *116*, 417−429.
(13) Lockless, S. W.; Ranganathan, R. Evolutionally conserved pathways of energetic connectivity in protein families. *Science* **1999**, *286*, 295−299.
(14) Shiau, A. K.; Barstad, D.; Radek, J. T.; Meyers, M. J.; Nettles, K. W.; Katzenellenbogen, B. S.; Katzenellenbogen, J. A.; Agard, D. A.; Greene, G. L. Structural characterization of a subtype-selective ligand reveals a novel mode of estrogen receptor antagonism. *Nat. Struct. Biol.* **2002**, *9*, 359−364.
(15) Nettles, K. W.; Sun, J.; Radek, J. T.; Sheng, S.; Rodriguez, A. L.; Katzenellenbogen, J. A.; Katzenellenbogen, B. S.; Greene, G. L. Allosteric control of ligand selectivity between estrogen receptors alpha and beta: implications for other nuclear receptors. *Mol. Cell* **2004**, *13*, 317−327.
(16) Sunn, K. L.; Cock, T.-A.; Crofts, L. A.; Eisman, J. A.; Gardiner, E. M. *Mol. Endocrinol.* **2001**, *15*, 1599−1609.
(17) Choi, M.; Yamamoto, K.; Itoh, T.; Makishima, M.; Mangelsdorf, D. J.; Moras, D.; DeLuca, H. F.; Yamada, S. Interaction between Vitamin D Receptor and Vitamin D Ligands. Two-Dimensional Alanine Scanning Mutational Analysis. *Chem. Biol.* **2003**, *10*, 261−270.
(18) Choi, M.; Yamamoto, K.; Masuno, H.; Nakashima, K.; Taga, T.; Yamada, S. Ligand Recognition by the Vitamin D Receptor. *Bioorg. Med. Chem.* **2001**, *9*, 1721−1730.
(19) Rochel, N.; Wurtz, J. M.; Mitschler, A.; Klaholz, B.; Moras, D. The Crystal Structure of the Nuclear Receptor for Vitamin D Bound to Its Natural Ligand. *Mol. Cell* **2000**, *5*, 173−179.
(20) Vanhooke, J. L.; Benning, M. M.; Bauer, C. B.; Pike, J. W.; DeLuca, H. F. Molecular Structure of the Rat Vitamin D Receptor Ligand Binding Domain Complexed with 2-Carbon-Substituted Vitamin D_3 Hormone Analogues and a LXXLL-Containing Coactivator Peptide. *Biochemistry* **2004**, *43*, 4101−4110.
(21) Tocchini-Valentini, G.; Rochel, N.; Wurtz, J.-M.; Moras, D. Crystal Structures of the Vitamin D Nuclear Receptor Liganded with the Vitamin D Side Chain Analogues Calcipotriol and Seocalcitol, Receptor Agonists of Clinical Importance. Insights into a Structural Basis for the Switching of Calcipotriol to a Receptor Antagonist by Further Side Chain Modification. *J. Med. Chem.* **2004**, *47*, 1956−1961.
(22) Tocchini-Valentini, G.; Rochel, N.; Wurtz, J. M.; Mitschler, A.; Moras, D. Crystal structures of the vitamin D receptor complexed to super agonist 20-epi ligands. *Proc. Natl. Acad. Sci. U.S.A.* **2001**, *98*, 5491−5496.
(23) Mi, L. Z.; Devarakonda, S.; Harp, J. M. Han, Q.; Pellicciari, R.; Willson, T. M.; Khorasanizadeh, S.; Rastinejad, F. Structural Basis for Bile Acid Binding and Activation of the Nuclear Receptor FXR. *Mol. Cell* **2003**, *11*, 1093−1100.
(24) Kitaura, K.; Ikeo, E.; Asada, T.; Nakano, T.; Uebayasi, M. Fragment molecular orbital method: an approximate computational method for large molecule. *Chem. Phys. Lett.* **1999**, *313*, 701−706.
(25) Nakano, T.; Kaminuma, T.; Sato, T.; Akiyama, Y.; Uebayasi, M.; Kitaura, K. Fragment Molecular Orbital Method: Application to polypepties, *Chem. Phys. Lett.* **2000**, *318*, 614−618.
(26) Ciesielski, F.; Rochel, N.; Mitschler, A.; Kouzmenko, A.; Moras, D. Structural investigation of the ligand binding domain of the zebrafish VDR in complexes with 1α,25$(OH)_2D_3$ and Gemini: purification crystallization and preliminary X-ray diffraction analysis. *J. Steroid Biochem. Mol. Biol.* **2004**, *89*−*90*, 55−59.
(27) Yamamoto, K.; Sun, W.-Y.; Ohta, M.; Hamada, K.; DeLuca, H. F.; Yamada, S. Conformationally restricted analogs of 1α,25-dihydroxyvitamin D_3 and its 20-epimer: Compounds for study of the three-dimensional structure of vitamin D responsible for binding to the receptor. *J. Med. Chem.* **1996**, *39*, 2727−2737.
(28) Shevde, N. K.; Plum, L. A.; Clagett-Dame, M.; Yamamoto, H.; Pike, J. W.; DeLuca, H. F. A potent analog of 1α,25-dihydroxyvitamin D_3 selectively induces bone formation. *Proc. Natl. Acad. Sci. U.S.A.* **2002**, *99*, 13487−13491.
(29) Makishima, M.; Lu, T. T.; Xie, W.; Whitfield, G. K.; Domoto, H.; Evans, R. M.; Haussler, M. R.; Mangelsdorf, D. J. Vitamin D receptor as an intestinal bile acid sensor. *Science* **2002**, *296*, 1313−1316.
(30) Herdick, M.; Steinmeyer, A.; Carlberg, C. Carboxylic ester antagonists of 1α,25-dihydroxyvitamin D_3 show cell-specific actions. *Chem. Biol.* **2000**, *7*, 885−894.
(31) Shiau, A. K.; Barstad, D.; Loria, P. M.; Cheng, L.; Kushner, P. J.; Agard, D. A.; Greene, G. L. The structural basis of estrogen receptor/coactivator recognition and the antagonism of this interaction by tamoxifen. *Cell* **1998**, *95*, 927−937.
(32) Geller, D. S.; Farhi, A.; Pinkerton, N.; Fradley, M.; Moritz, M.; Spitzer, A.; Meinke, G.; Tsai, F. T. F.; Sigler, P. B.; Lifton, R. P. Activating Mineralocorticoid Receptor Mutation in Hypertension Exacerbated by Pregnancy. *Science* **2000**, *289*, 119−123.
(33) Ishizuka, S.; Miura, D.; Ozono, K.; Chokki, C.; Mimura, H.; Norman, A. W. Antagonistic Actions *in Vivo* of (23S)-25-Dehydro-1α-Hydroxyvitamin D_3–26,23-Lactone on Calcium Metabolism Induced by 1α,25-Dihydroxyvitamin D_3. *Endocrinology* **2001**, *142*, 59−67.
(34) Ozono, K.; Saito, M.; Miura, D.; Michigami, T.; Nakajima, S.; Ishizuka, S. Analysis of the Molecular Mechanism for the Antagonistic Action of a Novel 1α,25-Dihydroxyvitamin D_3 Analogue toward Vitamin D Receptor Function. *J. Biol. Chem.* **1999**, *274*, 32376−32381.
(35) Whitfield, G. K.; Selznick, S. H.; Haussler, C. A.; Hsieh, J. C.; Galligan, M. A.; Jurutka, P. W.; Thompson, P. D.; Lee, S. M.; Zerwekh, J. E.; Haussler, M. R. Vitamin D receptors from patients with resistance to 1,25-dihydroxyvitamin D_3: point mutations confer reduced transactivation in response to ligand and impaired interaction with the retinoid X receptor heterodimeric partner. *Mol. Endocrinol.* **1996**, *10*, 1617−1631.
(36) Yamamoto, K.; Masuno, H.; Choi, M.; Nakashima, K.; Taga, T.; Ooizumi, H.; Umesono, K.; Sicinska, W.; VanHooke, J.; DeLuca, H. F.; Yamada, S. Three-dimensional modeling of and ligand docking to vitamin D receptor ligand binding domain. *Proc. Natl. Acad. Sci. U.S.A.* **2000**, *97*, 1467−1472.

JM050795Q